Measurement of transmission line parameters of three-core power cables with common earth screen

Published in IET Science, Measurement and Technology
Received on 10th July 2009
Revised on 17th December 2009
doi: 10.1049/iet-smt.2009.0062

ISSN 1751-8822

Measurement of transmission line parameters of three-core power cables with common earth screen

P. Wagenaars[1] *P.A.A.F. Wouters*[1] *P.C.J.M. van der Wielen*[2] *E.F. Steennis*[1,2]

[1]*Eindhoven University of Technology, P.O. Box 513, 5600 MB Eindhoven, The Netherlands*
[2]*KEMA, P.O. Box 9035, 6800 ET Arnhem, The Netherlands*
E-mail: p.wagenaars@tue.nl

Abstract: In power cables fast transient signals arise because of partial discharges. These signals propagate to the cable ends where they can be detected for diagnostic purposes. To enable optimal detection sensitivity and to judge their severity the propagation parameters Z_c (characteristic impedance) and γ (propagation coefficient) need to be known. A three-core power cable with a single metallic earth screen around the assembly of the cores has multiple, coupled propagation modes with corresponding characteristic impedances and propagation coefficients. This paper presents a practical method to measure and analyse the cable parameters. The propagation modes are decoupled into a modal solution. The modal solution is interpreted in terms of convenient propagation modes: a shield-to-phase (SP) propagation mode between conductors and earth screen and two identical phase-to-phase (PP) modes between conductors. The measurement method, based on a pulse response measurement, to determine all transmission line parameters of the SP and PP modes is proposed and tested on a cable sample. The model is validated by predicting the time, shape and amplitude of multiple reflections in all modes resulting from an injected pulse.

1 Introduction

In order to study and predict the propagation of partial discharge (PD) pulses in underground power cables a model of the power cable is required. Such models can for example be used for an online PD monitoring system for medium voltage power cables [1–3]. Location of the PD origin is established by measuring the difference in time-of-arrival at the cable ends and the location accuracy depends on the knowledge of the PD signal propagation velocity. The PD magnitude and waveform of the measured signal at the cable ends can be traced back only if the propagation characteristics are known. For high-frequency phenomena, such as PDs, a long homogeneous structure such as an underground power cable can be modelled as a transmission line [4, 5]. A transmission line can be characterised by two parameters: the characteristic impedance Z_c and the propagation coefficient γ. The propagation coefficient incorporates both the attenuation coefficient α and the propagation velocity v_p.

A single-core power cable can be modelled as a two-conductor transmission line with a single propagation mode. For single-core cables methods to measure Z_c and γ of a cable sample have been described, e.g. [6–9]. Literature on three-core power cables as transmission lines is scarce. There are many designs of this type of cable [10, 11], differing in the insulation used and additional layers applied for electric field control and protection against water ingress. A common cable design applies a metallic earth screen around each individual core. For such a design the cores can be modelled as three uncoupled two-conductor transmission lines. A belted paper-insulated lead-covered (PILC) cable, however, has a single metallic earth screen around the assembly of the cores. Some

doi: 10.1049/iet-smt.2009.0062

three-core cross-linked polyethylene (XLPE) cable designs also apply only a single metallic earth screen around the assembly of the three cores. Such configurations have multiple propagation modes and must be analysed as a multiconductor transmission line [12]. A PD occurring in the insulation will, depending of the location, induce a current in multiple modes. Therefore it is important to know the properties of all modes. Also the measurement methods from the earlier mentioned references cannot be applied directly to measure the parameters of three-core cables with common earth screen.

This paper describes the analysis of the propagation modes in a three-core cable with common earth screen, including decoupling them into three independent propagation modes and interpretation of these modes. The focus of this paper is a practical method to measure the transmission line parameters of all propagation channels, based on the pulse response of injected pulses. The measurement method is applied on a three-core XLPE cable with common earth screen and the results are presented.

2 Three-core cables with common earth screen

One of the oldest designs of a three-core power cable with common earth screen is the belted PILC cable. Even though nowadays they are rarely used in new cable circuits, in many countries the majority of the currently installed distribution-class cables are still PILC cables. A belted PILC cable has three phase conductors with paper insulation wrapped around them. A belt of paper insulation is then wrapped around the assembly of the three cores. A lead earth screen is applied around the belt. Around the lead sheath several additional layers are applied, but these layers have no influence on the propagation of signals through the cable. A schematic drawing of the relevant parts is depicted in Fig. 1.

Modern medium and high-voltage power cables generally use XLPE insulation. There are various constructions of three-core XLPE cables. The most common design equips each core with its own metallic earth screen. From a transmission-line-modelling point-of-view, each core can be regarded as a single-core XLPE cable and is therefore outside the scope of this paper. Some cable types do not apply a metallic earth screen around each individual core. Instead, a single metallic earth screen is applied around the assembly of the three cores. Each core does have its own semiconducting screen and swelling tapes. The metallic earth screen usually consists of helically wound copper wires. In Fig. 2, a schematic drawing of such a design is depicted.

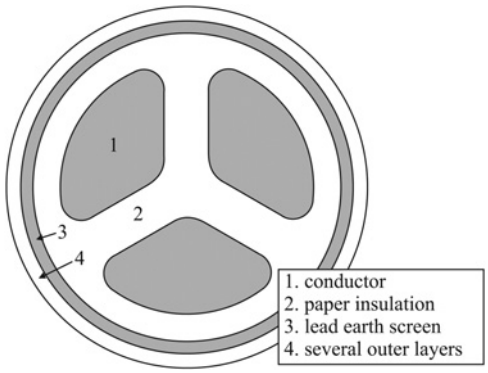

Figure 1 *Typical construction of belted PILC cable*

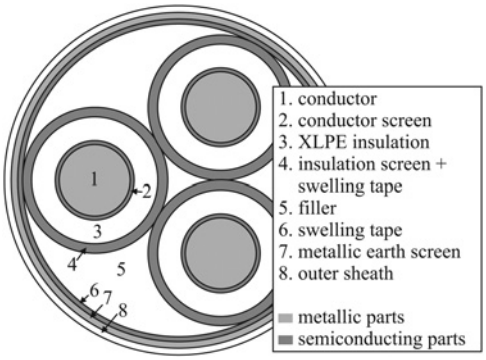

Figure 2 *Typical construction of three-core XLPE cable with common earth screen*

3 Multiconductor transmission line model

General multiconductor transmission line theory can be found in many textbooks, for example [12–14]. This section summarises the multiconductor transmission line analysis specific for a three-core power cable with common earth screen. Such a cable has three identical conductors that have cyclic symmetry with respect to the common earth screen, which serves as the reference conductor. Owing to this rotational symmetry of the three conductors the impedance matrix $\boldsymbol{Z}$ has only two unique values. The self-impedances Z_s on the diagonal have equal values and all mutual impedances Z_m, the off-diagonal elements, are equal. For the admittance matrix $\boldsymbol{Y}$ the same considerations apply. The self and mutual impedances and admittances are a function of the cable geometry and material properties. They are frequency dependent and incorporate effects such as skin and proximity effect, increased inductance because of the helical lay of the wire earth screen and dielectric losses in the insulation and semiconducting layers.

3.1 Telegrapher's equations

A three-core power cable has three conductors and a metallic earth screen, which serves as the reference/ground conductor. The frequency-domain voltages on and currents through the three-core conductors at position z along the transmission line are defined as column vectors $\boldsymbol{V}$ and $\boldsymbol{I}$

$$\boldsymbol{V} = \left(V_1, \quad V_2, \quad V_3\right)^{\mathrm{T}}$$
$$\boldsymbol{I} = \left(I_1, \quad I_2, \quad I_3\right)^{\mathrm{T}} \tag{1}$$

where V_i is the voltage on the ith conductor and I_i is the current through the ith conductor. The differential equations describing the voltages and currents at position z, sometimes referred to as Telegrapher's equations, are

$$\begin{aligned}\frac{\partial}{\partial z}\boldsymbol{V}(z) &= -\boldsymbol{Z}\boldsymbol{I}(z)\\ \frac{\partial}{\partial z}\boldsymbol{I}(z) &= -\boldsymbol{Y}\boldsymbol{V}(z)\end{aligned} \tag{2}$$

where $\boldsymbol{Z}$ is the (3 × 3) per-unit-length impedance matrix, and $\boldsymbol{Y}$ the (3 × 3) per-unit-length admittance matrix

$$\boldsymbol{Z} = \begin{pmatrix} Z_s & Z_m & Z_m \\ Z_m & Z_s & Z_m \\ Z_m & Z_m & Z_s \end{pmatrix}, \quad \boldsymbol{Y} = \begin{pmatrix} Y_s & Y_m & Y_m \\ Y_m & Y_s & Y_m \\ Y_m & Y_m & Y_s \end{pmatrix} \tag{3}$$

3.2 Modal analysis

One of the frequently used methods to decouple (2) applies a transformation matrix [12, 15]. Let the mode voltages $\boldsymbol{V}_m$ and currents $\boldsymbol{I}_m$ be defined as

$$\begin{aligned}\boldsymbol{V} &\stackrel{\text{def}}{=} \boldsymbol{T}_V\boldsymbol{V}_m\\ \boldsymbol{I} &\stackrel{\text{def}}{=} \boldsymbol{T}_I\boldsymbol{I}_m\end{aligned} \tag{4}$$

where $\boldsymbol{T}_I$ and $\boldsymbol{T}_V$ are transformation matrices that define the transformation between the voltages and currents of the individual conductors to the modal quantities. From (2) and (4) the wave equations for the modal voltages and currents are obtained

$$\begin{aligned}\frac{\partial^2}{\partial z^2}\boldsymbol{V}_m(z) &= \boldsymbol{T}_V^{-1}\boldsymbol{Z}\boldsymbol{Y}\boldsymbol{T}_V\boldsymbol{V}_m(z) = \boldsymbol{Z}_m\boldsymbol{Y}_m\boldsymbol{V}_m(z)\\ \frac{\partial^2}{\partial z^2}\boldsymbol{I}_m(z) &= \boldsymbol{T}_I^{-1}\boldsymbol{Y}\boldsymbol{Z}\boldsymbol{T}_I\boldsymbol{I}_m(z) = \boldsymbol{Y}_m\boldsymbol{Z}_m\boldsymbol{I}_m(z)\end{aligned} \tag{5}$$

where $\boldsymbol{Z}_m = \boldsymbol{T}_V^{-1}\boldsymbol{Z}\boldsymbol{T}_I$ and $\boldsymbol{Y}_m = \boldsymbol{T}_I^{-1}\boldsymbol{Y}\boldsymbol{T}_V$. The transformation matrices $\boldsymbol{T}_V$ and $\boldsymbol{T}_I$ should be chosen such that the equations become decoupled, that is the matrices $\boldsymbol{T}_V^{-1}\boldsymbol{Z}\boldsymbol{Y}\boldsymbol{T}_V$ and $\boldsymbol{T}_I^{-1}\boldsymbol{Y}\boldsymbol{Z}\boldsymbol{T}_I$ are diagonal. The columns of $\boldsymbol{T}_V$ are the eigenvectors of $\boldsymbol{Z}\boldsymbol{Y}$ and the columns of $\boldsymbol{T}_I$ the eigenvectors of $\boldsymbol{Y}\boldsymbol{Z}$ [12, 15]. We choose a set of eigenvectors corresponding to two distinct eigenvalues, of which one is two-fold degenerate, such that we obtain convenient propagation modes. The transformations matrices are given by

$$\boldsymbol{T}_V = \begin{pmatrix} 1 & \frac{1}{3} & \frac{1}{3} \\ 1 & -\frac{2}{3} & \frac{1}{3} \\ 1 & \frac{1}{3} & -\frac{2}{3} \end{pmatrix}, \quad \boldsymbol{T}_I = \begin{pmatrix} \frac{1}{3} & \frac{2}{3} & \frac{2}{3} \\ \frac{1}{3} & -\frac{4}{3} & \frac{2}{3} \\ \frac{1}{3} & \frac{2}{3} & -\frac{4}{3} \end{pmatrix} \tag{6}$$

These transformation matrices decompose the propagation modes in a three-core power cable with common earth screen into three uncoupled modes: the shield-to-phase (SP) mode and two phase-to-phase (PP) modes. The SP mode travels in the propagation channel between shield and the three phases together.

The voltage V_{sp} and current I_{sp} of this mode are defined as

$$\begin{aligned}V_{sp} &\stackrel{\text{def}}{=} \frac{1}{3}(V_1 + V_2 + V_3)\\ I_{sp} &\stackrel{\text{def}}{=} I_1 + I_2 + I_3\end{aligned} \tag{7}$$

The voltage $V_{pp,1}$ and current $I_{pp,1}$ of the first PP channel is defined as

$$\begin{aligned}V_{pp,1} &\stackrel{\text{def}}{=} V_1 - V_2\\ I_{pp,1} &\stackrel{\text{def}}{=} \frac{1}{2}(I_1 - I_2)\end{aligned} \tag{8}$$

The voltage $V_{pp,2}$ and current $I_{pp,2}$ of the second PP channel are the same except that V_2 and I_2 are replaced by, respectively, V_3 and I_3. Applying $\boldsymbol{T}_V$ and $\boldsymbol{T}_I$ to (4) verifies that the modal voltages and current are equal to the defined SP and PP channels: $\boldsymbol{V}_m = (V_{sp}, V_{pp,1}, V_{pp,2})^T$ and $\boldsymbol{I}_m = (I_{sp}, I_{pp,1}, I_{pp,2})^T$.

3.3 Characteristic impedance and propagation coefficient

The solution of the differential equations in (5) is a superposition of forward and backward travelling waves

$$\begin{aligned}\boldsymbol{V}_m(z) &= \mathrm{e}^{-\boldsymbol{\gamma}_m z}\boldsymbol{V}_m^+(0) + \mathrm{e}^{\boldsymbol{\gamma}_m z}\boldsymbol{V}_m^-(0)\\ \boldsymbol{I}_m(z) &= \mathrm{e}^{-\boldsymbol{\gamma}_m z}\boldsymbol{I}_m^+(0) + \mathrm{e}^{\boldsymbol{\gamma}_m z}\boldsymbol{I}_m^-(0)\end{aligned} \tag{9}$$

where the diagonal transmission coefficient matrix $\boldsymbol{\gamma}_m$ is given by

$$\boldsymbol{\gamma}_m = \sqrt{\boldsymbol{Y}_m\boldsymbol{Z}_m} = \sqrt{\boldsymbol{Z}_m\boldsymbol{Y}_m} \tag{10}$$

The relation between voltage and current for the forward or backward travelling waves is given by the characteristic impedance matrix $\boldsymbol{Z}_c$

$$\boldsymbol{V} = \boldsymbol{Z}_c\boldsymbol{I} \tag{11}$$

Similarly, a diagonal modal characteristic impedance matrix $\boldsymbol{Z}_{c,m}$ can be defined

$$\boldsymbol{V}_m = \boldsymbol{Z}_{c,m}\boldsymbol{I}_m \tag{12}$$

which is related to $\boldsymbol{Z}_c$ according

$$\boldsymbol{Z}_{c,m} = \boldsymbol{T}_V^{-1}\boldsymbol{Z}_c\boldsymbol{T}_I \tag{13}$$

The expressions for the SP and PP mode characteristic impedances and propagation coefficients can be obtained

doi: 10.1049/iet-smt.2009.0062

from the diagonal components of (9) and (12)

$$Z_{sp} = \frac{V_{sp}}{I_{sp}} \quad \text{with} \quad \begin{aligned} V_{sp}(z) &= e^{-\gamma_{sp} z} V_{sp}^{+}(0) + e^{\gamma_{sp} z} V_{sp}^{-}(0) \\ I_{sp}(z) &= e^{-\gamma_{sp} z} I_{sp}^{+}(0) - e^{\gamma_{sp} z} I_{sp}^{-}(0) \end{aligned} \tag{14}$$

$$Z_{pp} = \frac{V_{pp,k}}{I_{pp,k}} \quad \text{with} \quad \begin{aligned} V_{pp,k}(z) &= e^{-\gamma_{pp} z} V_{pp,k}^{+}(0) + e^{\gamma_{pp} z} V_{pp,k}^{-}(0) \\ I_{pp,k}(z) &= e^{-\gamma_{pp} z} I_{pp,k}^{+}(0) - e^{\gamma_{pp} z} I_{pp,k}^{-}(0) \end{aligned} \tag{15}$$

where k is either 1 or 2. Owing to the rotational symmetry both PP channels have equal transmission line parameters.

The normal characteristic impedance matrix $\boldsymbol{Z}_c$ in terms of the SP and PP impedances is obtained from (13)

$$\boldsymbol{Z}_c = \begin{pmatrix} Z_{sp} + \frac{1}{3}Z_{pp} & Z_{sp} - \frac{1}{6}Z_{pp} & Z_{sp} - \frac{1}{6}Z_{pp} \\ Z_{sp} - \frac{1}{6}Z_{pp} & Z_{sp} + \frac{1}{3}Z_{pp} & Z_{sp} - \frac{1}{6}Z_{pp} \\ Z_{sp} - \frac{1}{6}Z_{pp} & Z_{sp} - \frac{1}{6}Z_{pp} & Z_{sp} + \frac{1}{3}Z_{pp} \end{pmatrix} \tag{16}$$

3.4 Reflection and transmission coefficients

If a transmission line with characteristic impedance $\boldsymbol{Z}_c$ is terminated by load impedance $\boldsymbol{Z}_L$ an incoming wave will partially reflect on and partially transmit into the load impedance. The load impedance is not necessarily a discrete impedance, but can also be another transmission line. The reflection and transmission coefficients are calculated using the assumption that voltage and current are continuous at the interface

$$\begin{aligned} \boldsymbol{V}^{i} + \boldsymbol{V}^{r} &= \boldsymbol{V}^{t} \\ \boldsymbol{I}^{i} - \boldsymbol{I}^{r} &= \boldsymbol{I}^{t} \end{aligned} \tag{17}$$

where $\boldsymbol{V}^{i}$, $\boldsymbol{V}^{r}$, $\boldsymbol{V}^{t}$ are the voltages and $\boldsymbol{I}^{i}$, $\boldsymbol{I}^{r}$, $\boldsymbol{V}^{t}$ are the currents of the incident, reflected and transmitted waves, respectively. The polarity of the currents is taken positive in the travelling direction of the corresponding wave.

The voltage reflection and transmission coefficient matrices $\boldsymbol{\Gamma}_V$ and $\boldsymbol{\tau}_V$ are defined as

$$\boldsymbol{V}^{r} = \boldsymbol{\Gamma}_V \boldsymbol{V}^{i} \quad \text{and} \quad \boldsymbol{V}^{t} = \boldsymbol{\tau}_V \boldsymbol{V}^{i} \tag{18}$$

Applying (17) and (18) yields the reflection and transmission coefficient matrices

$$\boldsymbol{\Gamma}_V = (\boldsymbol{Z}_L - \boldsymbol{Z}_c)(\boldsymbol{Z}_L + \boldsymbol{Z}_c)^{-1} \quad \text{and} \quad \boldsymbol{\tau}_V = \boldsymbol{1} + \boldsymbol{\Gamma}_V \tag{19}$$

where $\boldsymbol{1}$ is the identity matrix.

4 Measurement method

The transmission line parameters of a single-core cable can be measured using a single-pulse response measurement, see appendix or [6]. Usually a calibration of the injection cable as described in the appendix is also required. In order to determine the parameters of the SP and PP channels of a three-core cable with common earth screen two-pulse response measurements are required. Both measurements are analysed as if it would concern a single-core cable, as described in the appendix, yielding a measured characteristic impedance $Z_{c,meas}$ and a measured propagation coefficient γ_{meas}. Since the pulse injection may simultaneously excite several modes the measured $Z_{c,meas}$ and γ_{meas} must be converted to the desired transmission line parameters of the SP and PP channels.

4.1 SP measurement

The first measurement yields the parameters of the SP channel. During the SP measurement the three conductors of the three-core cable are interconnected making the voltages on all three conductors equal ($V_1 = V_2 = V_3$) at the injection point. The central conductor of the (single-core) injection cable is connected to the three conductors of the three-core cable, while the outer shield of the injection cable is connected to the common earth screen of the three-core cable. The far end of the three-core cable is left open. The test setup is shown in Fig. 3

The first step is to perform the measurement procedure as described in the appendix, including calibration of injection cable and adapter. This measurement results in a measured characteristic impedance $Z_{c,meas}$ and propagation coefficient γ_{meas}. These parameters are related to SP channel parameters Z_{sp} and γ_{sp}. In order to determine this relationship the injection cable is most conveniently described as if it is a three-core cable. The central conductor of the single-core injection cable can be interpreted as three separate conductors in direct contact. A current through either conductor results in an equal voltage on all three conductors. Therefore all values of the characteristic impedance matrix must be equal. Additionally, the shield-to-phase impedance Z_{sp} (14) is equal to the characteristic impedance of the injection cable $Z_{c,inj}$. This results in following characteristic impedance matrix for the injection cable during this measurement

$$\boldsymbol{Z}_{c,inj} = \begin{pmatrix} Z_{c,inj} & Z_{c,inj} & Z_{c,inj} \\ Z_{c,inj} & Z_{c,inj} & Z_{c,inj} \\ Z_{c,inj} & Z_{c,inj} & Z_{c,inj} \end{pmatrix} \tag{20}$$

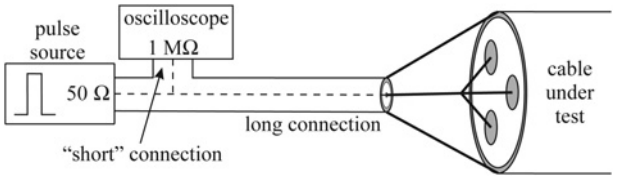

Figure 3 *Setup for SP measurement*

where $Z_{c,inj}$ is the characteristic impedance of the injection cable 50 Ω.

The voltages of the first reflected pulse are given by

$$\boldsymbol{V}^{r1} = \boldsymbol{\Gamma}_V \boldsymbol{V}^{i} \tag{21}$$

where $\boldsymbol{V}^{i}$ are incident voltages and $\boldsymbol{\Gamma}_V$ the reflection coefficient matrix (19) with $\boldsymbol{Z}_c$ the characteristic impedance matrix of the injection cable (20) and $\boldsymbol{Z}_L$ the characteristic impedance matrix of the three-core cable under test (16). The transfer function from the injected pulse $\boldsymbol{V}^{i}$ to the first reflection $\boldsymbol{V}^{r1}$ is

$$H_1 = \frac{\boldsymbol{V}^{r1}(k)}{\boldsymbol{V}^{i}(k)} = \frac{Z_{sp} - Z_{c,inj}}{Z_{sp} + Z_{c,inj}} \tag{22}$$

where k indicates the kth element of the voltage vector. Its value is either 1, 2 or 3; all three values yield the same result. This transfer function corresponds to the measured H_1 in (38), yielding

$$Z_{c,meas} = Z_{sp} \tag{23}$$

The second reflection $\boldsymbol{V}^{r2}$ is the pulse that has propagated back and forth once through the three-core cable under test. The voltages of this pulse are given by

$$\boldsymbol{V}^{r2} = \boldsymbol{\tau}_V^{-} \boldsymbol{T}_V \mathrm{e}^{-\gamma_m 2l_c} \boldsymbol{T}_V^{-1} \boldsymbol{\tau}_V^{+} \boldsymbol{V}^{i} \tag{24}$$

where l_c is the length of the cable under test, $\boldsymbol{\tau}_V^{+}$ the voltage transmission coefficient matrix from injection cable to three-core cable (i.e. from (20) to (16)), and $\boldsymbol{\tau}_V^{-}$ the voltage transmission coefficient matrix from three-core cable to injection cable (i.e. from (16) to (20)). Since the far end is open pulses arriving at the far end reflect unaffected. The transfer function to the second reflection is obtained from either element of (24)

$$H_2 = \frac{\boldsymbol{V}^{r2}(k)}{\boldsymbol{V}^{i}(k)} = \frac{4 Z_{c,inj} Z_{sp}}{(Z_{c,inj} + Z_{sp})^2} \mathrm{e}^{-\gamma_{sp} 2l_c} \tag{25}$$

Combining this transfer function with (41) shows that the measured propagation coefficient corresponds to the SP mode

$$\gamma_{meas} = \gamma_{sp} \tag{26}$$

The results for Z_{sp} and γ_{sp} are trivial in the sense that the system can also be considered as a 50 Ω injection cable connected to a single-core power cable with impedance Z_{sp}. For the PP mode the result is less obvious.

Because the measurement of the SP parameters is basically the same as a pulse response measurement on a single-core cable, the measured SP parameters have the same accuracy as the parameters acquired with a pulse response measurement on a single-core cable. The appendix contains a discussion on the accuracy of the pulse response measurement.

4.2 PP measurement

A direct measurement of the PP channel requires simultaneous injection of two equal pulses with opposite polarity, along with a differential detection. A more practical option is to connect the central conductor of the injection cable to one conductor of the three-core cable. The other two conductors are floating, meaning that they have an approximately infinite impedance to the environment. In Fig. 4, the test setup is depicted. An incident pulse will couple to both the SP and the PP channel of the three-core cable. As with the SP measurement a propagation measurement is conducted as if the cable under test is a single-core cable (see the appendix) yielding a measured characteristic impedance $Z_{c,meas}$ and propagation coefficient γ_{meas}. These parameters are converted to the parameters of the PP channel.

Again, the injection circuit, consisting of the single-core injection cable connected to one phase, is interpreted as a three-core cable. The single-core injection cable is connected to one phase of the three-core cable, making $\boldsymbol{Z}_{c,inj}(1, 1)$ equal to the characteristic impedance of the injection cable. The other two phases of the three-core cable are floating, as if they are connected to an infinite impedance Z_∞. Therefore $\boldsymbol{Z}_{c,inj}(2, 2)$ and $\boldsymbol{Z}_{c,inj}(3, 3)$ are Z_∞. Since there is no coupling between the injection cable and the infinite impedances the off-diagonal impedances are zero. This results in the following characteristic impedance matrix of the injection cable for this configuration

$$\boldsymbol{Z}_{c,inj} = \begin{pmatrix} Z_{c,inj} & 0 & 0 \\ 0 & Z_\infty & 0 \\ 0 & 0 & Z_\infty \end{pmatrix} \tag{27}$$

Similar to the SP measurement the reflection coefficient matrix $\boldsymbol{\Gamma}_V$ is calculated using (16) and (27). The transfer function of the injected pulse to the first reflection is

$$H_1 = \lim_{Z_\infty \to \infty} \frac{\boldsymbol{V}^{r1}(1)}{\boldsymbol{V}^{i}(1)} = \frac{(1/3)Z_{pp} + Z_{sp} - Z_{c,inj}}{(1/3)Z_{pp} + Z_{sp} + Z_{c,inj}} \tag{28}$$

Combining this transfer function with (38)

$$Z_{c,meas} = \frac{1}{3} Z_{pp} + Z_{sp} \tag{29}$$

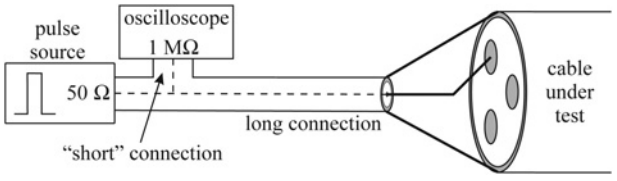

Figure 4 *Setup for PP measurement*

doi: 10.1049/iet-smt.2009.0062

The characteristic impedance of the PP channel is given by

$$Z_{pp} = 3(Z_{c,meas} - Z_{sp}) \tag{30}$$

The second reflection is calculated using (24) with (27) for the impedance of the injection circuit. The measured transfer function is

$$H_2 = \lim_{Z_\infty \to \infty} \frac{\boldsymbol{V}^{r2}(1)}{\boldsymbol{V}^{i}(1)} = \frac{4Z_{c,inj}}{(Z_{c,inj} + Z_{c,meas})^2}\left(\frac{1}{3}Z_{pp}e^{-\gamma_{pp}2l_c} + Z_{sp}e^{-\gamma_{sp}2l_c}\right) \tag{31}$$

Combining this transfer function with (41) gives for the measured propagation coefficient

$$e^{-\gamma_{meas}2l_c} = \frac{e^{-\gamma_{pp}2l_c}Z_{pp} + 3e^{-\gamma_{sp}2l_c}Z_{sp}}{Z_{pp} + 3Z_{sp}} \tag{32}$$

The propagation coefficient of the PP channel can be calculated from the measured γ_{meas} using

$$e^{-\gamma_{pp}2l_c} = e^{-\gamma_{meas}2l_c}\frac{Z_{pp} + 3Z_{sp}}{Z_{pp}} - e^{-\gamma_{sp}2l_c}\frac{3Z_{sp}}{Z_{pp}} \tag{33}$$

The PP parameters Z_{pp} and γ_{pp} are calculated from the results of two measurements. Therefore the errors accumulate in Z_{pp} and γ_{pp}. The accumulation of the errors depends on the values of the SP and PP parameters of the cable under test. For example, for the three-core XLPE power cable used in the experiments presented in the next section the relative error in Z_{pp} is approximately twice as large as the relative error in Z_{sp}. The relative error in α_{pp} is 2–2.5 times larger than the relative error in α_{sp}, and the relative error in $v_{p,pp}$ is approximately 6 times larger than the relative error in $v_{p,sp}$.

5 Experiments

5.1 Measurement of SP and PP parameters of XLPE cable

The measurement method described in the previous section has been applied on a cable sample on a drum. The tested cable is a three-core XLPE cable with common earth screen, as depicted in Fig. 2. The rated voltage is 6/10 kV, the conductors are $3 \times 240\ mm^2$ aluminium and the length is 351 m. The characteristic impedance Z_c and propagation coefficient γ of the SP and PP channels have been measured using the method described in the previous section. The pulse source (HP 33120A Function Generator) generates a rectangular pulse with a width of 115 ns, which is injected via an RG223 50 Ω coaxial cable of 50 m. Signals are recorded using a 12 bit, 60 MS/s digitizer (Spectrum MI.3033). To increase the signal-to-noise ratio each measurement is repeated 1000× and the measured waveforms are averaged. The measured characteristic impedances are plotted in Fig. 5. The measured propagation coefficients are split into the attenuation coefficient $\alpha = \mathrm{Re}(\gamma)$, plotted in Fig. 6, and propagation velocity $v_p = \omega/\mathrm{Im}(\gamma)$, plotted in Fig. 7.

The characteristic impedance and attenuation show a sharp peak near 8.5 MHz because of an experimental artefact caused by the fact that the injected pulse (width ≃1/8.5 MHz) has no energy around that frequency range. Above approximately 7 MHz the experimentally determined values for the attenuation α and propagation velocity v_p become unreliable anyway, since higher frequencies are strongly attenuated after travelling back and forth through the power cable.

5.2 Validation using XLPE cable measurements

The propagation velocities of the SP and PP channels are not the same because of the presence of the semiconducting layers. The second reflection v^{r2} of the PP measurement

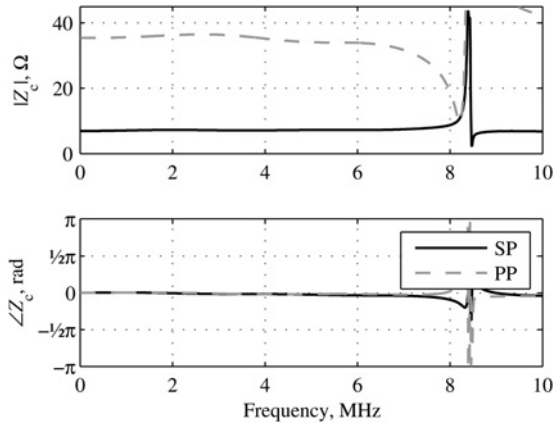

Figure 5 *Measured characteristic impedance Z_c of SP and PP channels*

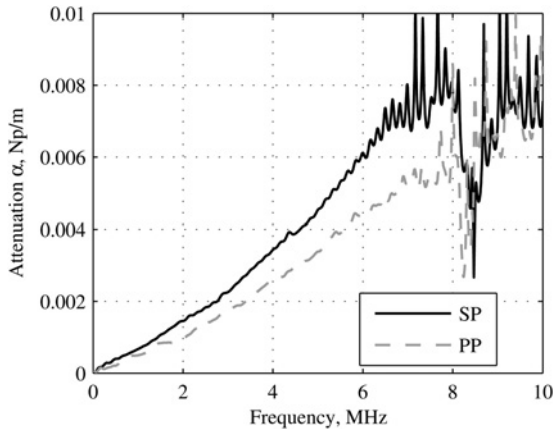

Figure 6 *Measured attenuation coefficient α of SP and PP channels*

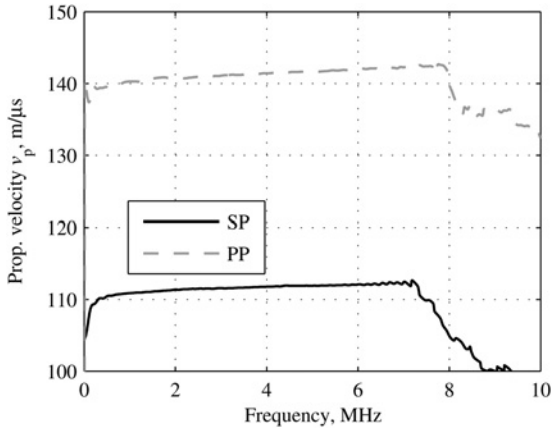

Figure 7 *Measured propagation velocity v_p of SP and PP channels*

consists of two distinct pulses, see Fig. 8, the first pulse travelled through the PP channel and the second through the SP channel.

As a validation the reflections observed during the PP measurement are simulated using the equations from Section 3, the measured injected pulse v^i, the measured calibration parameters H_{inj} and Z_{adpt}, the measured characteristic impedances Z_{sp} and Z_{pp} and the measured propagation coefficients γ_{sp} and γ_{pp}. The simulated response is plotted in Fig. 8 together with the measured signal. The first and second reflections match perfectly because the transmission line parameters where derived from the part of the measured waveform containing these pulses. The predictions of the third, fourth and higher-order reflections, on the other hand, are a good validation since all aspects of the model and measurement method are involved in the shape of these reflections, including the different propagation velocities of the SP and PP channels. The multiple reflected pulses of the SP and PP modes mix at each reflection from the three-core cable on the injection cable. The measured waveform (incorporating the propagation velocities as well as the amplitudes depending on the impedances) is accurately predicted by the cable model simulation.

On the same cable another measurement, similar to the PP measurement, is performed. For this measurements the two conductors that are not connected to the injection cable are earthed, while during the PP measurement they are floating (see Fig. 9). Again, the measured injected pulse v^i, the calibration parameters H_{inj} and Z_{adpt}, the characteristic impedances Z_{sp} and Z_{pp} and the propagation coefficients γ_{sp} and γ_{pp} are used to predict successive reflections. The PP parameters are not derived from this measurement, but taken from the PP measurement presented in the previous paragraph. Therefore all reflections serve as validation of the model and the SP and PP parameters. The sequence of signal reflections is predicted accurately. The only significant difference between the prediction and the measurement is the small pulse in the measured signal at $t = 12$ µs. The same difference, but much smaller, can be observed at $t = 17$ µs. The simulated signals lack this pulse most likely because in the model the earth connections of the two conductor are a perfect short circuit. In reality, the short circuits have a small impedance, and there may be a coupling between the phases. If in the model small self and/or mutual inductances are introduced, a pulse appears at that point in time, whereas the rest of the simulated signal is unaffected.

5.3 Validation using PILC cable measurements

Another validation measurement is performed on a belted PILC cable with a rated voltage of 12.5/12.5 kV, 3×95 mm^2 copper conductors and a length of 201 m. An SP and PP measurements are conducted to determine the parameters of the SP and PP channels. These parameters are combined with the measured injected pulse v^i to simulate all reflections observed during the PP measurement. The measured and simulated signals are plotted in Fig. 10. Because the first two reflections (v^{r1} and v^{r2}) of the measurement are used to determine Z_{pp} and

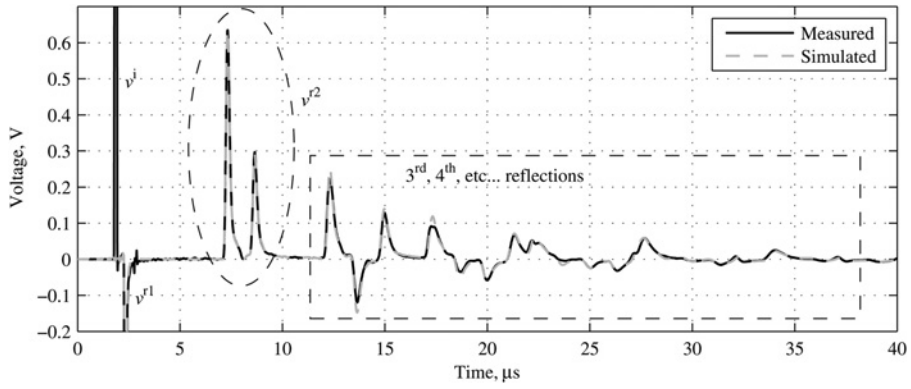

Figure 8 *Measured and simulated signals of PP measurement (with two conductors floating) on three-core cable with XLPE insulation*

IET Sci. Meas. Technol., 2010, Vol. 4, Iss. 3, pp. 146–155
doi: 10.1049/iet-smt.2009.0062

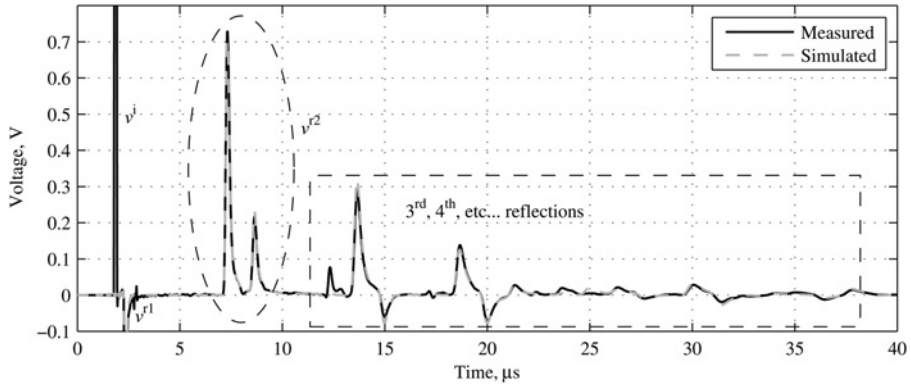

Figure 9 *Measured and simulated signals of PP measurement (with two conductors earthed) on three-core cable with XLPE insulation*

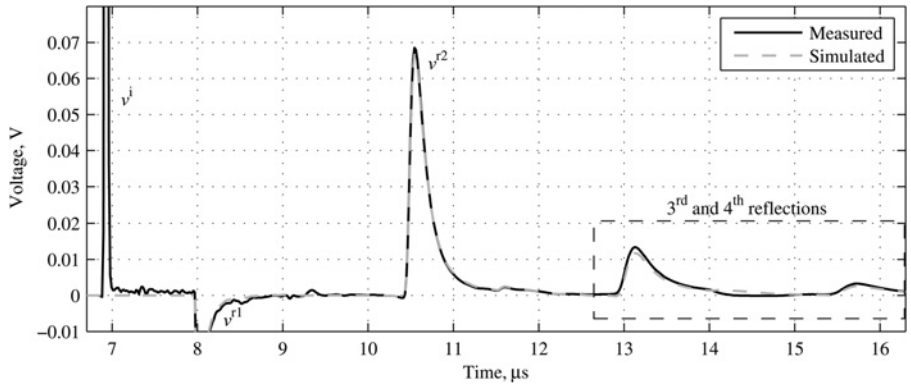

Figure 10 *Measurement and simulated signals of PP measurement (with two conductors floating) on belted PILC cable*

γ_{pp}, the simulation matches the measurement for these two pulses. The third and fourth reflections are accurately predicted by the model.

6 Conclusions

The propagation modes in a three-core cable with common earth screen can be interpreted as three uncoupled modes. One mode travels between the three conductors and earth screen. The other two modes travel between two conductors and have identical transmission line parameters. The transmission line parameters of the two different propagation channels of such a cable can be assessed by two-pulse response measurements. In the first measurement, a pulse is injected in all phases with respect to ground and the SP parameters are obtained. In the second measurement, a signal is injected in only one phase (and the other two are left floating). From this measurement and the earlier obtained SP parameters the PP characteristics can be calculated.

The analysis of the propagation modes in a three-core power cable with common earth screen, including decoupling them into convenient SP and PP modes, allows researchers to study the propagation of high-frequency phenomena through this type of cable. This includes the transmission and reflection of waveforms at the cable ends. The presented measurement method, consisting of two-pulse response measurements, is a practical method to fully determine the transmission line parameters of a three-core cable with common earth screen. Both measurement method and model were successfully validated on an XLPE power cable sample. Very detailed prediction of multiple reflections was achieved including the mixing of propagation modes having distinct propagation velocities.

7 Acknowledgments

The authors thank KEMA Nederland B.V. and the Dutch utilities Alliander N.V., Stedin B.V. and Enexis B.V. for supporting this research.

8 References

[1] VAN DER WIELEN P.C.J.M., VEEN J., WOUTERS P.A.A.F., STEENNIS E.F.: 'On-line partial discharge detection of MV cables with defect localisation (pdol) based on two time synchronised sensors'. Proc. Int. Conf. Electricity Distrib. (CIRED), Turin, Italy, June 2005, session no. 1

[2] VAN DER WIELEN P.C.J.M., STEENNIS E.F.: 'Experiences with continuous condition monitoring of in-service mv cable

connections'. Proc. Power Eng. Soc. (PES) Power Systems Conf. & Exp. (PSCE), Seattle, WA, USA, March 2009

[3] MICHEL M.: 'Innovative asset management and targeted investments using on-line partial discharge monitoring & mapping techniques'. Proc. 19th Int. Conf. Electricity Distrib. (CIRED), Vienna, Austria, May 2007, p. 0551

[4] SADIKU M.N.O.: 'Elements of electromagnetics' (Oxford University Press, 2001, 3rd edn.)

[5] POPOVIĆ Z., POPOVIĆ B.D.: 'Introductory electromagnetics' (Prentice-Hall, 2000)

[6] PAPAZYAN R., ERIKSSON R.: 'Calibration for time domain propagation constant measurements on power cables', *IEEE Trans. Instrum. Meas.*, 2003, **52**, (2), pp. 415–418

[7] PAPAZYAN R., PETTERSSON P., EDIN H., ERIKSSON R., GÄFVERT U.: 'Extraction of high frequency power cable characteristics from s-parameter measurements', *IEEE Trans. Dielectr. Electr. Insul.*, 2004, **11**, (3), pp. 461–470

[8] VILLEFRANCE R., HOLBØLL J.T., HENRIKSEN M.: 'Estimation of medium voltage cable parameters for PD-detection'. Conf. Rec. IEEE Int. Symp. Electrical Insulation (ISEI), Arlington, VA, USA, June 1998, pp. 109–112

[9] VAN DER WIELEN P.C.J.M.: 'On-line detection and location of partial discharges in medium-voltage power cables'. PhD thesis, Eindhoven University of Technology, 2005

[10] BARTNIKAS R., SRIVASTAVA K.D.: 'Power and communication cables: theory and applications' (McGraw-Hill, 2000)

[11] MOORE G.F. (ED.): 'Electric cables handbook' (Blackwell Science Ltd, 1997, 3rd edn.)

[12] PAUL C.R.: 'Analysis of multiconductor transmission lines' (Wiley, 1994, 1st edn.)

[13] FRANKEL S.: 'Multiconductor transmission line analysis' (Artech House, Inc., 1977)

[14] FACHE N., OLYSLAGER F., DE ZUTTER D.: 'Electromagnetic and circuit modelling of multiconductor transmission lines' (Clarendon Press, 1993)

[15] PAUL C.R.: 'Decoupling the multiconductor transmission line equations', *IEEE Trans. Microw. Theory Tech.*, 1996, **44**, (8), pp. 1429–1440

9 Appendix

A pulse response measurement [6] can be used to determine the (characteristic) impedance of a device under test. For a cable this includes the propagation coefficient. For a pulse response measurement a pulse source is attached to a matching cable (e.g. 50 Ω). The signals are recorded with an oscilloscope using the 1 MΩ input impedance at a short distance from the pulse source. This configuration ensures that the input impedance of the combination of the pulse source and the oscilloscope matches the impedance of the injection cable. Furthermore, their connection is sufficiently short to prevent signal distortion because of reflections between the pulse source and oscilloscope. The cable under test (CUT) is connected to the far end of the injection cable. The injection cable is chosen longer than the pulse width so that injected and reflected pulses can be separated in time domain. The setup is depicted in Fig. 11.

Upon an injected pulse the following pulses are recorded by the oscilloscope: v^{i} injected pulse, v^{r1} reflection on transfer from injection cable to CUT, v^{r2} reflection on far end of the CUT. These pulses are cut out from the recorded signal and converted to frequency domain. Two transfer function are extracted from these pulses

$$H_1 = \frac{V^{\mathrm{r1}}}{V^{\mathrm{i}}} \quad \text{and} \quad H_2 = \frac{V^{\mathrm{r2}}}{V^{\mathrm{i}}} \tag{34}$$

The transfer functions are not only affected by the CUT, but also by the injection cable and the adapter that connects the injection cable to the CUT. Therefore two calibration measurements are conducted to determine their influence. First, the injection cable is shorted at the far end. A pulse is injected and the transfer function $H_{\mathrm{cal1}} = V^{\mathrm{r1}}/V^{\mathrm{i}}$ from injected to reflected pulse is calculated. The voltage reflection coefficient on the short is -1. The transfer function H_{cal1} is corrected for this reflection coefficient yielding the transfer function representing the influence of the injection cable H_{inj}

$$H_{\mathrm{inj}} = -H_{\mathrm{cal1}} \tag{35}$$

Next, the adapter series impedance Z_{adpt} is determined by connecting the injection cable to the power cable using the adapter and short-circuiting the conductor and shield at the interface between adapter and CUT. The transfer function from injected to reflected pulse of this calibration measurement is

$$H_{\mathrm{cal2}} = \frac{V^{\mathrm{r1}}}{V^{\mathrm{i}}} = H_{\mathrm{inj}}\Gamma_V = H_{\mathrm{inj}}\frac{Z_{\mathrm{adpt}} - Z_{\mathrm{c,inj}}}{Z_{\mathrm{adpt}} + Z_{\mathrm{c,inj}}} \tag{36}$$

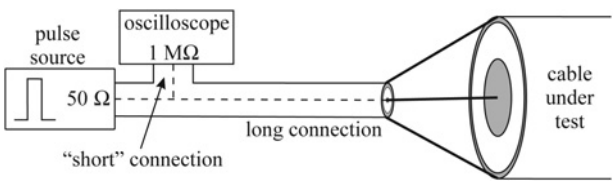

Figure 11 *Pulse response measurement setup*

doi: 10.1049/iet-smt.2009.0062

The value of the adapter impedance Z_{adpt} is given by

$$Z_{adpt} = Z_{c,inj}\frac{H_{inj} + H_{cal2}}{H_{inj} - H_{cal2}} \tag{37}$$

where $Z_{c,inj}$ is the characteristic impedance of the injection cable. As an indication for typical Z_{adpt} values: during the SP measurement of the experiment in Section 5 the adapter impedance Z_{adpt} was approximately an inductance of 60 nH.

For the actual pulse response measurement the short from the previous measurement is removed. Now, the injection cable is connected to the CUT via the adapter and Z_{adpt} acts as e series impedance in the circuit. Injecting a pulse results in a signal with multiple reflections. The first reflection is required to determine the characteristic impedance $Z_{c,meas}$, and the second reflection is required to determine the propagation coefficient γ_{meas}. The characteristic impedance of the CUT is derived from the transfer function $H_1 = V^{r1}/V^{i}$ and the earlier calibrated H_{inj} and Z_{adpt}

$$Z_{c,meas} = Z_{c,inj}\frac{H_{inj} + H_1}{H_{inj} - H_1} - Z_{adpt} \tag{38}$$

The second reflection V^{r2} is the pulse that was injected, transmitted to the power cable reflected on the open far end of the power cable and transmitted back to the injection cable. The transfer function of the injected pulse to the second reflection is given by

$$H_2 = \frac{V^{r2}}{V^{i}} = H_{inj}\tau_V^{+}e^{-\gamma 2l_c}\tau_V^{-} \tag{39}$$

where l_c is the length of the CUT, τ_V^{+} the voltage transmission coefficient from injection cable to CUT and τ_V the voltage transmission coefficient from CUT to injection cable. The voltage transmission coefficients are given by

$$\tau_V^{+} = \frac{2Z_{c,meas}}{Z_{c,inj} + Z_{adpt} + Z_{c,meas}} \tag{40a}$$

$$\tau_V^{-} = \frac{2Z_{c,inj}}{Z_{c,inj} + Z_{adpt} + Z_{c,meas}} \tag{40b}$$

The propagation coefficient γ_{meas} can be calculated from the measurements

$$e^{-\gamma_{meas}2l_c} = \frac{H_2}{H_{inj}\tau_V^{+}\tau_V^{-}} \tag{41}$$

The accuracy of the (indirectly) measured transmission line parameters ($Z_{c,meas}$ and γ_{meas}) depends on many factors, such as: accuracy of the equipment, length of the cable under test, length of the injection cable, noise level, characteristic impedance of the cable under test and the method of isolating the pulses from the recorded signal. A complete analysis of the accumulation of errors in all these parameters on the accuracy of the transmission line parameters is beyond the scope of this paper. For an indication of the accuracies that can be achieved in practice see [6, 9]. In [6], the results of a pulse response measurements are converted to the S_{21} scattering parameter and compared to a network analyser measurement. Because the S_{21} parameter is influenced by both $Z_{c,meas}$ and γ_{meas}, it gives an indication for the accuracy of both parameters. The maximum error of the pulse response measurements on short cable samples ($<$50 m) is 2.1%. In [9], pulse response measurements and network analyser measurements are performed on a 200 m cable. The maximum error in $Z_{c,meas}$ is approximately 10%. The γ_{meas} is split in a real part, the attenuation α and an imaginary part, the propagation velocity v_p. Below 1 MHz the maximum error in α is 25%, above 1 MHz the maximum error is less than 10%. For the propagation velocity the maximum error is less than 0.5%. Owing to the long length of the cable under test the pulse response measurement has a high accuracy for v_p.